Dynamic Simulation of Differential-Driven Mobile Robot Taking into Account the Friction Between the Wheel and the Road Surface

Trinh Thi Khanh Ly, Hoang Thien, Dam Khac Nhan, and Nguyen Hong Thai

Abstract The dynamics problem is essential in designing dynamic control laws for tracking autonomous mobile robots (AMR). Differential-driven mobile robots (DDMR) among AMR are commonly researched and applied. Thus, this article focuses on modelling and simulating the dynamics of a DDMR when moving on an arbitrary trajectory. The reverse dynamics model of a DDMR is established, taking into account the sliding phenomenon between the wheel and the road surface. The coefficient of friction is determined experimentally based on a platform DDMR and an S-type load cell. NURBS interpolation is used to design the motion trajectory of the DDMR in the general case. The research results have important implications for designing kinematics and dynamics controllers for the DDMR to follow a complex trajectory without slipping at a certain speed.

Keywords Differential-drive mobile robot · Dynamic modeling · Simulation · NURBS curve · Friction

1 Introduction

Mobile robots (MBs) are being widely applied in many different fields, such as in industrial logistics [1], medical logistics [2], tunnelling robots in mining [3], or service restaurant service [4]. MBs were one of the important elements in the industrial production system 4.0 [4–7]. Modeling dynamics is a significant problem when

T. T. K. Ly · D. K. Nhan
Faculty of Automation Technology, Electric Power University (EPU), Hanoi, Vietnam

H. Thien · N. H. Thai (✉)
School of Mechanical Engineering, Hanoi University of Science and Technology (HUST), Hanoi, Vietnam
e-mail: thai.nguyenhong@hust.edu.vn

B. T. Long et al. (eds.), *Proceedings of the 3rd Annual International Conference on Material, Machines and Methods for Sustainable Development (MMMS2022)*, Lecture Notes in Mechanical Engineering,
https://doi.org/10.1007/978-3-031-31824-5_44

designing, manufacturing, and controlling MBs. There have been many studies on the dynamics of different types of MBs [8–10]. Ren et al. [11] modelled and simulated an open-loop dynamics controller of an omnidirectional MB with three wheels, ignoring wheel slip and friction between the wheels with the working environment. Sarkar et al. [12] proposed a feedback nonlinear dynamics controller that follows the trajectory according to the Dubins method with the assumption of ignoring slip and friction. Several other studies have tried to design different controllers to improve the position and posture accuracy of MBs during movement with the assumption that there is no friction between the wheel and road surface [13–16]. Zamanian et al. [17] modelled the dynamics problem of a 4-wheel MB taking into account the longitudinal and transverse sliding when moving on arbitrary sloped surfaces, Sidek et al. [18] proposed a nonlinear dynamics controller to improve the lateral slip of a DDMR when navigating an MB. Cerkala et al. [19] modelled the frictional states in the newton dynamics model to design a PI controller that follows the trajectory is a second-order curve similar are some other studies [20, 21], etc. In the above studies, in which friction between wheel and road surface is assumed, have the disadvantage of not being close to practice.

In this work, a dynamic model for a DDMR was established considering the friction between the wheel and road surface with variable load. In addition, a complex curve was applied when the coefficient of friction was determined experimentally based on a platform robot manufactured as input data for the simulation problem.

2 Mathematical Models of Dynamics

2.1 *Kinematic Model*

Consider a DDMR moving along the trajectory ξ with no longitudinal slip in the global coordinate $\vartheta_f\{O_f\ x_f\ y_f\ z_f\}$ as described in Fig. 1. According to [22], the kinematic of the DDMR is defined by:

$$\begin{cases} V_G = (V_2 + V_1)/2 = r(\dot{\varphi}_2 + \dot{\varphi}_1)/2 \\ \Omega = (V_2 - V_1)(2\ell)^{-1} = r(\dot{\varphi}_2 - \dot{\varphi}_1)(2\ell)^{-1} \end{cases} \tag{1}$$

The linear velocity of the robot in the global coordinate is determined by:

$$\mathbf{q}_\mathrm{f} = \begin{bmatrix} x_G & y_G & \theta \end{bmatrix}^T = \begin{bmatrix} \cos\theta & \sin\theta & 0 \\ 0 & 0 & 1 \end{bmatrix}^T \begin{bmatrix} V_G \\ \Omega \end{bmatrix} \tag{2}$$

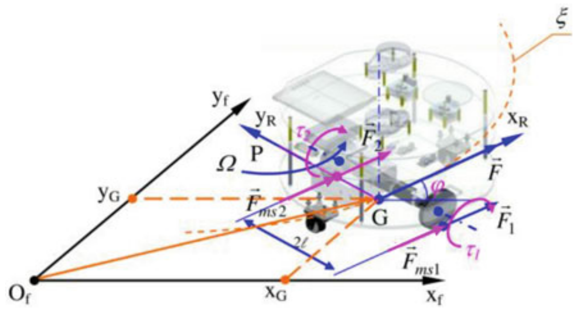

Fig. 1 Illustrate the kinematic relationship of DDMR in the global coordinate

2.2 The Dynamic Model of DDMR

If τ_1, τ_2 are the torque of the left and right driving wheels; F_{ms1}, F_{ms2} are the friction force between the two wheels and the road surface; m_p is the mass of the robot; m_w is the wheel's mass; I_p, I_w, I_m are the moment of inertia of the robot, the wheel about its axis and the wheel around its diameter, respectively. Applying Lagrange dynamics equation we have the dynamic equation of the DDMR is given by:

$$\begin{cases} m\ddot{x}_G - \lambda_1 \sin\theta + (\lambda_2 + \lambda_3)\cos\theta = 0 \\ m\ddot{y}_G + \lambda_1 \cos\theta + (\lambda_2 + \lambda_3)\sin\theta = 0 \end{cases}; \quad I\ddot{\theta} + \ell(\lambda_3 - \lambda_2) = 0;$$
$$\begin{cases} I_w\ddot{\varphi}_1 - \lambda_2 r = \tau_1 - rF_{ms1} \\ I_w\ddot{\varphi}_2 - \lambda_3 r = \tau_2 - rF_{ms2} \end{cases} \quad (3)$$

wherein $m = m_p + 2m_w$; $I = I_p + 2m_w\ell^2 + 2I_m$; λ_1, λ_2 and λ_3 are Lagrange multipliers.

Writing Eq. (3) in the form of an algebraic matrix, we have [23]:

$$\mathbf{D}(\mathbf{q})\ddot{\mathbf{q}} + \mathbf{M}^T(\mathbf{q})\boldsymbol{\lambda} = \mathbf{E}(\boldsymbol{\tau} - \mathbf{F}), \quad \mathbf{q} = [x_G, y_G, \theta, \varphi_1, \varphi_2]^T \quad (4)$$

Transform Eq. (4) using the matrix $\mathbf{B}(\mathbf{q})$ with $\mathbf{v}(t) = \begin{bmatrix} V_G & \Omega \end{bmatrix}^T$, we have the dynamics of DDMR when considering the frictional force:

$$\overline{\mathbf{D}}(\mathbf{q})\dot{\mathbf{v}}(t) + \overline{\mathbf{C}}(\mathbf{q})\mathbf{v}(t) = \overline{\mathbf{E}}(\boldsymbol{\tau} - \mathbf{F}), \quad \mathbf{B}(\mathbf{q}) = \begin{bmatrix} \cos\theta & \sin\theta & 0 & r^{-1} & r^{-1} \\ 0 & 0 & 1 & -\ell r^{-1} & \ell r^{-1} \end{bmatrix}^T \quad (5)$$

3 Simulation Results and Discussion

3.1 Setting Simulation Parameters

Step 1. *Determine the inertia parameters of DDMR*

Inertia parameters matrix of the DDMR, the frames, and the wheel are determined from the design by the Mass Properties tool of Solidworks software, given by:

$$\mathbf{I}_r = \begin{bmatrix} 0.128 & -0.001 & -0.004 \\ -0.001 & 0.130 & 0.007 \\ -0.004 & 0.007 & 0.142 \end{bmatrix}, \ \mathbf{I}_t = \begin{bmatrix} 0.114 & -0.001 & -0.004 \\ -0.001 & 0.126 & 0.007 \\ -0.004 & 0.007 & 0.131 \end{bmatrix},$$
$$\mathbf{I}_b = \begin{bmatrix} 0.153 \times 10^{-3} & 0 & 0 \\ 0 & 0.299 \times 10^{-3} & 0 \\ 0 & 0 & 0.153 \times 10^{-3} \end{bmatrix} \tag{6}$$

Step 2. *Experimental determination of the coefficient of friction of the driving wheel with the road surface*

Experimental determination of the coefficient is carried out according to the diagram Fig. 3, with the platform as described in Fig. 2, has the parameters: DDMR mass $m = 10.4$ (kg), driving wheel radius $r = 0.0475$ (m), the distance between two driving wheels $2\ell = 0.3$ (m).

Experimental process is carried out with 3 cases: (1) No load, (2) Test load with $m_{L1} = 1$ kg and (3) Test load with $m_{L2} = 2$ kg. For each test case 10 times. The experimental data is described in Table 1.

With the experimental values in Table 1, the coefficient of friction between the wheel and the road surface is calculated by the formula below:

Fig. 2 A photo of the platform DDMR

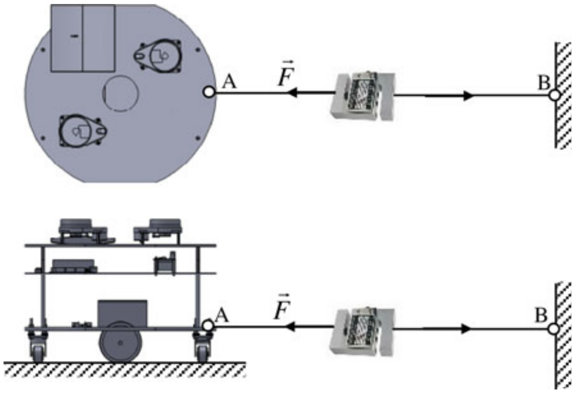

Fig. 3 Determine the coefficient of friction

Table 1 Experimental data determine the coefficient of friction

No.	Case 1	Case 2	Case 3	No.	Case 1	Case 2	Case 3
	F_1 (kgf)	F_2 (kgf)	F_3 (kgf)		F_1 (kgf)	F_2 (kgf)	F_3 (kgf)
1	3.535	4.060	4.490	6	3.560	4.020	4.570
2	3.570	4.130	4.520	7	3.565	4.035	4.550
3	3.550	4.160	4.485	8	3.570	4.015	4.525
4	3.535	4.150	4.520	9	3.565	4.035	4.520
5	3.570	4.075	4.545	10	3.550	4.120	4.525

The average value: **Case 1**: 3.557, **Case 2**: 4.080, **Case 3**: 4.525

$$\mu_i = F_{tb}(m_\Sigma g)^{-1},\ \mu_c = \mu_{tb} = (\mu_{kt} + \mu_{t1} + \mu_{t2})3^{-1} \tag{7}$$

where F_{tb} is the mean force value, $m_\Sigma = m + m_{Li}$ (i = 1, 2); g = 9.81 m/s^2.

Thus, the coefficient of friction between the wheel and the road surface is $\mu_c =$ 0.355.

Step 3. *Simulated trajectory settings*

To simulate DDMR dynamics in the general case, we use the NURBS curve [23, 24] to design the motion trajectory of the DDMR, as shown in Fig. 4, B_i points (i = 1–10) are NURBS interpolation points. The red curve is the motion trajectory of DDMR after performing NURBS interpolation on Matlab software.

Step 4. *Set the kinematics and dynamics parameters*

From the motion trajectory ξ is defined in Fig. 4, the radius of curvature of the trajectory is obtained as follows:

$$\rho(t) = \left|\left(\dot{x}(t)^2 + \dot{y}(t)^2\right)^{3/2}(\dot{x}(t)\ddot{y}(t) - \dot{y}(t)\ddot{x}(t))^{-1}\right| \tag{8}$$

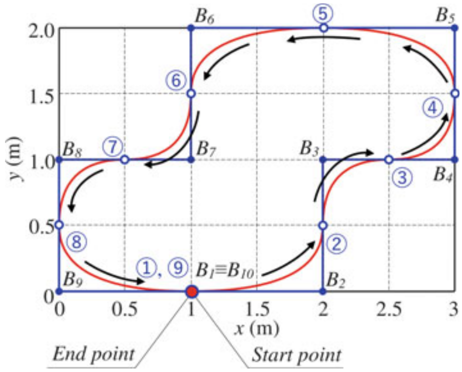

Fig. 4 Motion trajectory of DDMR

Here $(x(t), y(t))$ is the coordinates of trajectory ξ.

Set the linear velocity V_G of the DDMR $V_G = 0.2$ (m/s). Thus, the angular velocity and angular acceleration of the DDMR is determined by:

$$\Omega(t) = 2V_G\rho^{-1}(t),\ \varepsilon(t_i) = \dot{\Omega}(t_i) = \Delta\Omega(t_i)(\Delta t_i)^{-1} = (\Omega(t_{i+1}) - \Omega(t_i))(t_{i+1} - t_i)^{-1} \tag{9}$$

3.2 Simulation Results and Discussion

From the kinematics and dynamics equations established in Sect. 2 and the setting parameters are presented in Sect. 3.1. Figure 5 is a calculation diagram simulating the dynamics problem of DDMR set up on Simulink of Matlab software. Figure 6 is a graph describing the angular velocity and acceleration of the DDMR with the markers corresponding to those in Fig. 4.

The simulation results in Fig. 6 shown at inflexion points 2, 3, 6, and 7 in Fig. 4 have curvature radii 0.954 m, 0.988 m, 0.988 m, and 0.978 m, respectively, angular velocity of DDMR has a sudden jump from positive to negative or vice versa. That leads to an abrupt change of moment τ_1, τ_2 as described in Fig. 7. While at inflexion points 1, 5 with corresponding curvature radii of 4.0 m, 3.950 m, and no change of direction τ_1, τ_2 at that time is a point on the smooth curve. At inflexion points 4, 8 have curvature radii of 0.628 m and 0.499 m and no change of direction. From the simulation results and discussion above, it can be seen that at inflexion points with the change of direction of DDMR, the angular velocity has jumped, causing the driving torque of the driving wheels to change suddenly, causing the slip phenomenon.

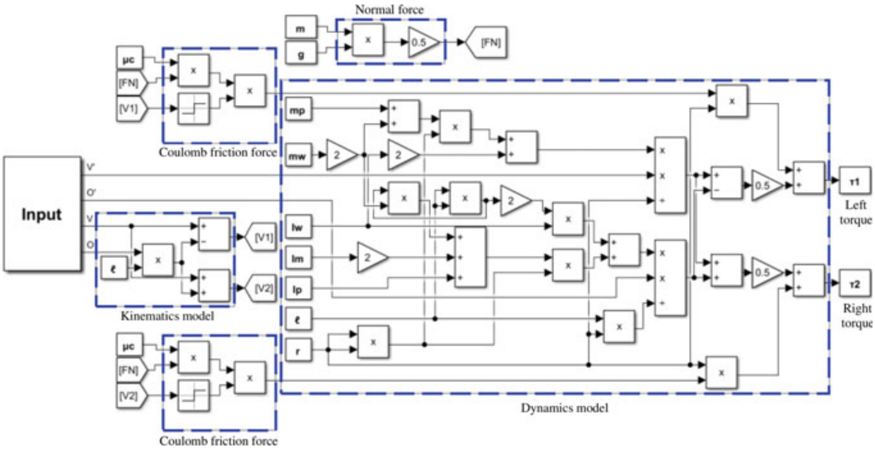

Fig. 5 Simulink diagram calculates dynamic simulation for DDMR

Fig. 6 The velocity and acceleration angular of DDMR

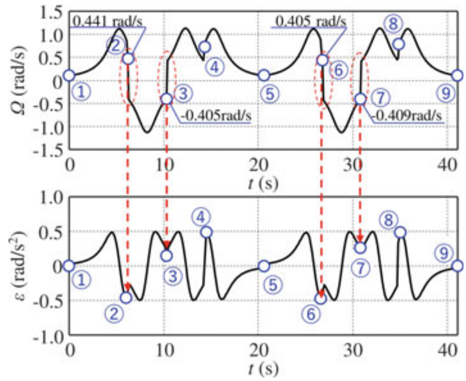

Fig. 7 Torque value of two driving wheels for DDMR

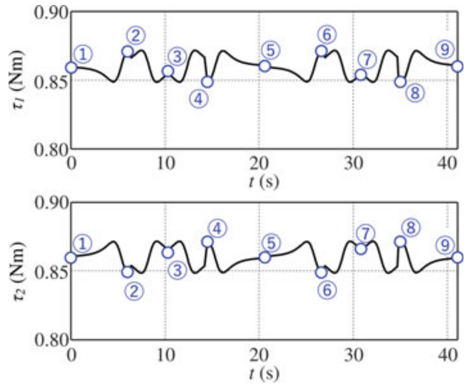

4 Conclusion

From simulation results, experimental, discussion above, this research has achieved the following results: (i) The dynamics problem with a simple friction model is considered in the case of DDMR moving along a general trajectory; (ii) At inflexion points with a small radius of curvature and DDMR, there is a change of direction, resulting in a sudden change in torque. At that time, there is a slippage between the wheel and the road surface, causing the position and posture error of the DDMR. These results have scientific significance in designing trajectory tracking dynamics controllers for practical DDMRs such as AGVs serving logistics in industry or hospitals. However, the limitation of this research is that it has not considered the influence of rough and material homogeneity of the road surface in practice on the coefficient of friction. These factors affect the ability to grip the road and the motion accuracy of DDMR. As such, it will be considered part of our future research goals.

Acknowledgements Hoang Thien was funded by the Master Scholarship Programme of Vingroup Innovation Foundation (VINIF), code VINIF.2022.ThS.128.

References

1. Cardarelli E, Digani V, Sabattini L, Secchi C, Fantuzzi C (2017) Cooperative cloud robotics architecture for the coordination of multi-AGV systems in industrial warehouses. Mechatronics 45:1–13
2. Søraa RA, Fostervold ME (2021) Social domestication of service robots: the secret lives of automated guided vehicles (AGVs) at a Norwegian hospital. Int J Hum Comput Stud 152:102627
3. Nguyen TH, Nguyen TQ (2017) A kinematic control algorithm for blasthole drilling robotic arm in tunneling. Sci Technol Dev J 20(K5):13–22
4. Shimmura T, Ichikari R, Okuma T, Ito H, Okada K, Nonaka T (2020) Service robot introduction to a restaurant enhances both labor productivity and service quality. Procedia CIRP 88:589–594
5. Thai NH, Trinh LTK, Dzung LQ (2021) Roadmap, routing and obstacle avoidance of AGV robot in the static environment of the flexible manufacturing system with matrix devices layout. Sci Technol Dev J 24(3):2091–2099
6. Ahmadi SM, Taghadosi MB, AmirReza Haqshenas M (2021) A state augmented adaptive backstepping control of wheeled mobile robots. Trans Inst Meas Control 43(2):434–445
7. Ly TTK, Thai NH, Dzung LQ, Thanh NT (2020) Determination of kinematic control parameters of omnidirectional AGV robot with mecanum wheels track the reference trajectory and velocity. In: Sattler KU, Nguyen DC, Vu NP, Long BT, Puta H (eds) Advances in engineering research and application. ICERA 2020. Lecture notes in networks and systems, vol 178, pp 319–328
8. Yu R, Ding S, Tian H, Chen Y-H (2021) A hierarchical constraint approach for dynamic modeling and trajectory tracking control of a mobile robot. J Vib Control, 1–13
9. Andaluz VH, Roberti F, Carelli R, Toibero JM, Wagner B (2011) Adaptive dynamic path following control of an unicycle-like mobile robot. In: International conference on intelligent robotics and applications, pp 563–574
10. Vázquez JA, Villa MV (2008) Path-tracking dynamic model based control of an omnidirectional mobile robot. IFAC Proc 41(2):5365–5370

11. Ren C, Ma S (2013) Dynamic modeling and analysis of an omnidirectional mobile robot. In: IEEE/RSJ international conference on intelligent robots and systems, pp 4860–4865
12. Sarkar N, Yun X, Kumar V (1994) Control of mechanical systems with rolling constraints: application to dynamic control of mobile robots. Int J Robot Res 13(1):55–69
13. Thai NH, Ly TTK, Long NT, Dzung LQ (2021) Trajectory tracking using linear state feedback controller for a mecanum wheel omnidirectional. In: Khang NV, Hoang NQ, Ceccarelli M (eds) Advances in Asian mechanism and machine science. ASIAN MMS 2021. Mechanisms and machine science, vol 113, pp 411–421
14. Thai NH, Ly TTK (2022) Trajectory tracking control for mecanum wheel mobile robot by time-varying parameter PID controller. Bull Electr Eng Inf 11(4):1902–1910
15. Thai NH, Ly TTK (2022) Path tracking control for car-like robots by PID controller with time-varying parameters. Sci Technol Dev J 5(2)
16. Ly TTK, Thien H (2022) Bézier trajectory tracking control of the omnidirectional mobile robot based on a linear time-varying state feedback controller. Sci Technol Dev J 25(2):2444–2452
17. Zamanian H, Javidpour F (2016) Dynamic modeling, and simulation of 4-wheel skid-steering mobile robot with considering tires longitudinal and lateral slips. Int J Sci Res Knowl 4(2):040–055
18. Sidek N, Sarkar N (2008) Dynamic modeling and control of nonholonomic mobile robot with lateral slip. In: Third international conference on systems, pp 35–40
19. Čerkala J, Jadlovska A (2014) Mobile robot dynamics with friction in Simulink. In: Proceedings of the 22th annual conference proceedings of the international scientific conference—technical computing, Bratislava, pp 1–10
20. Xie Y, Zhang X, Meng W, Zheng S, Jiang L, Meng J, Wang S (2021) Coupled fractional-order sliding mode control and obstacle avoidance of a four-wheeled steerable mobile robot. ISA Trans, 282–294
21. Sun Z, Xie H, Zheng J, Man Z, He D (2021) Path-following control of mecanum-wheels omnidirectional mobile robots using nonsingular terminal sliding mode. Mech Syst Signal Process 147:107–128
22. Thai NH, Ly TTK, Thien H, Dzung LQ (2022) Trajectory tracking control for differential-drive mobile robot by a variable parameter PID controller. Int J Mech Eng Robot Res 11(8):614–621
23. Thai NH, Thien H, Ly TTK (2022) NURBS curve trajectory tracking control for differential-drive mobile robot by a linear state feedback dynamic controller. In: Le AT, Pham VS, Le MQ, Pham HL (eds) The AUN/SEED-Net joint regional conference in transportation, energy, and mechanical manufacturing engineering. RCTEMME 2021, pp 610–623
24. Thai NH, Ly TTK (2022) NURBS curve trajectory tracking control for differential-drive mobile robot by a linear state feedback controller. In: Nguyen DC, Vu NP, Long BT, Puta H, Sattler KU (eds) Advances in engineering research and application. ICERA 2021. Lecture notes in networks and systems, vol 366, pp 685–696